Chapter

# Urban Planning Using a Geospatial Approach: A Case Study of Libya

*Bahareh Kalantar, Husam A.H. Al-najjar, Hossein Mojaddadi Rizeei, Maruwan S.A.B. Amazeeq, Mohammed Oludare Idrees, Alfian Abdul Halin and Shattri Mansor*

## Abstract

Large scale developmental projects firstly require the selection of one or more cities to be developed. In Libya, the selection process is done by selected organizations, which is highly influenced by human judgement that can be inconsiderate of socioeconomic and environmental factors. In this study, we propose an automated selection process, which takes into consideration only the important factors for city (cities) selection. Specifically, a geospatial decision-making tool, free of human bias, is proposed based on the fuzzy overlay (FO) and technique for order performance by similarity to ideal solution (TOPSIS) techniques for development projects in Libya. In this work, a dataset of 17 evaluation criteria (GIS factors) across five urban conditioning factors were prepared. The dataset served as input to the FO model to calculate weights (importance) for each criterion. A support vector machine (SVM) classifier was then trained to refine weights from the FO model. TOPSIS was then applied on the refined results to rank the cities for development. Experimental results indicate promising overall accuracy and kappa statistics. Our findings also show that highest and lowest success rates are 0.94 and 0.79, respectively, while highest and lowest prediction rates are 0.884 and 0.673, respectively.

**Keywords:** fuzzy overlay, urban development, TOPSIS, Libya

## 1. Introduction

Rapid population growth and urbanization have caused many problems in the implementation of developmental projects in cities. Haphazard infrastructural project execution that includes disregard in prioritizing city (or cities) selection is also a factor hampering sustainable development practices. Development projects that rely on selected organizations, which in turn rely on human judgment, can lead to unrealistic criteria evaluation, causing delays in project execution [1]. However, the fact remains that continued infrastructure development is unavoidable, especially since urban cities constantly need to evolve and grow to keep up with the times [2].

The selection of a city (or a group of cities) is one of the most important steps for sustainable development. The selection criteria must ensure that the city (cities) has high priority for development and is (are) in line with the needs of the local citizens.

Moreover, timely selection requires effective planning and analysis and must consider multiple conflicting and disproportionate factors (such as those that have critical socioeconomic and environmental implications to different stakeholders). Urban planning application using remote sensing (RS) and geographical information systems (GIS) is one of the many areas that can be explored for city selection. Such applications would not only eliminate human bias but would also be able to make more objective decisions based on data.

### 1.1 Remote sensing and GIS applications in urban planning

Remote sensing can be applied in different aspects of urban planning such as (but not limited to) urban traffic analysis, urban environment analysis (air and water pollutions), and urban expansion. With recent developments in remote sensing technologies, remote sensing data can be exploited for urban studies. One example is the classification of land use based on high spatial and spectral resolution data such as orthomosaic and elevation images. Multidimensional spatiotemporal data can now be reliably obtained by sensors in different scale ranges and with flexible repetition rates [3].

### 1.2 Remote sensing sensors for urban planning

Medium- to high-resolution satellite imagery can be used by urban planners and land managers to monitor land conditions to support decision-making for sustainable urban development. Remote sensors are able to provide voluminous amounts of data, which can be exploited to produce/update GIS maps or for detection changes in urban land covers. High-resolution satellite sensors available on IKONOS, for example, can collect diverse geospatial data for studying vegetation. The sensors can sense 4 m resolution multispectral and 1 m resolution panchromatic, Quickbird imageries with 2.4 m resolution multispectral and 61 cm resolution panchromatic, and Worldview-4 imageries with 1.24 m resolution multispectral and 31 cm panchromatic. Medium-resolution satellite sensors, available on Landsat-8, Sentinel-2, and SPOT, are also valuable data sources for urban and vegetation change detection from various time periods during the same season, which further supports analyzing any past changes. Analysis of such data can then be used for decision-making and planning for further development of a particular urban area [4].

### 1.3 Integration of GIS and remote sensing for urban planning

Remote sensing data can be integrated with other spatial data to perform various types of full-fledged assessments. GIS techniques can be utilized to integrate the required spatial data and analytic data from various sources, such as field survey data, topographic maps, aerial photographs, and also archived data. The data can be represented as location (i.e., latitude and longitudes) or even as tabular attributes. GIS techniques play a substantial role in the data integration process of multilayer spatial information along with statistical information in various developmental scenarios [5].

### 1.4 Methods and approaches for urban planning

Multi-criteria decision-making (MCDM) is concerned with making a decision by evaluating multiple conflicting criteria. It embodies various methods and procedures where the gist is the formal incorporation of multiple conflicting criteria in the analytical process [6]. In the context of GIS, this refers to the spatial decision-making process based on GIS data with geolocation tags. Spatial decision-making techniques have been used to solve many GIS problems such as locating solar plants, urban planning, and project construction optimization [7]. Advanced MCDM methods include simple additive weighting (SAW) [8], analytic hierarchy process (AHP) [9], and TOPSIS [10]. Fuzzy set theory and random set theory are also MCDM techniques that incorporate sophisticated algorithms to resolve uncertainty in data [11–14].

TOPSIS is a MCDM technique that deals with real-world problems. It basically ranks criteria on the basis of the shortest distance from the positive ideal solution (PIS) and the farthest distance from the negative ideal solution (NIS) [15]. The work in [2] illustrates the application of a GIS-based MCDM tool for urban infrastructural planning. Awasthi et al. [16] presented a fuzzy TOPSIS method for selecting the best location for an urban distribution center in Canada. Uysal and Tosun [17] proposed a fuzzy TOPSIS-based maintenance management system using 17 criteria categorized under 5 contending parameters. The criteria were deduced from questionnaire feedbacks and interviews administered to company maintenance managers. In addition, Momeni et al. [18] presented a fuzzy TOPSIS-based method for maintenance strategy selection. Baysal et al. [19] developed a two-stage fuzzy method to determine the best sub-municipal projects among a set of proposed projects. The method simplifies the selection process and provides an objective decision outcome for stakeholders. Shelton and Medina [20] presented an integrated method to prioritize transportation projects in Wilmington Area, USA, based on multi-criteria decision support systems, AHP and TOPSIS methods. The process optimally selects the important routes that best serve the interest of the general public.

Based on the literature, TOPSIS has been successfully applied in many fields, producing reasonably accurate results. This study proposes an automated TOPSIS-based solution for prioritizing urban projects based on criteria that meet sustainable development. Specifically, this work addresses the following questions on the value of remote sensing (and GIS) to urban planning:

1. Which remotely sensed dataset(s) is (are) useful for urban planning?

2. Which criteria can be derived from remotely sensed data?

3. What are the major factors that need to be considered in urban developments?

From these questions, this study further looks at the automated prioritization of urban projects based on criteria that meet sustainable development practices. The specific objectives are (i) to identify factors that play major roles in urban development and (ii) to develop a geospatial solution based on TOPSIS for prioritizing projects for urban development.

## 2. Study area and preparation of the conditioning factors

This study focuses on Libya, a country in the Maghreb region of North Africa (**Figure 1**). Libya borders the Mediterranean Sea to the north and Egypt to the east. Along the southeast of Libya is Sudan, Chad. To the south is Niger. Algeria and Tunisia constitute the western border. Libya is the 17th largest nation in the world with a landmass of over 1,759,540 km$^2$. The study area in the northern part of Libya covers six districts, namely, Darnah, Al Jabal Al Akhdar, Benghazi, Al Marj, Al Qubbah, and

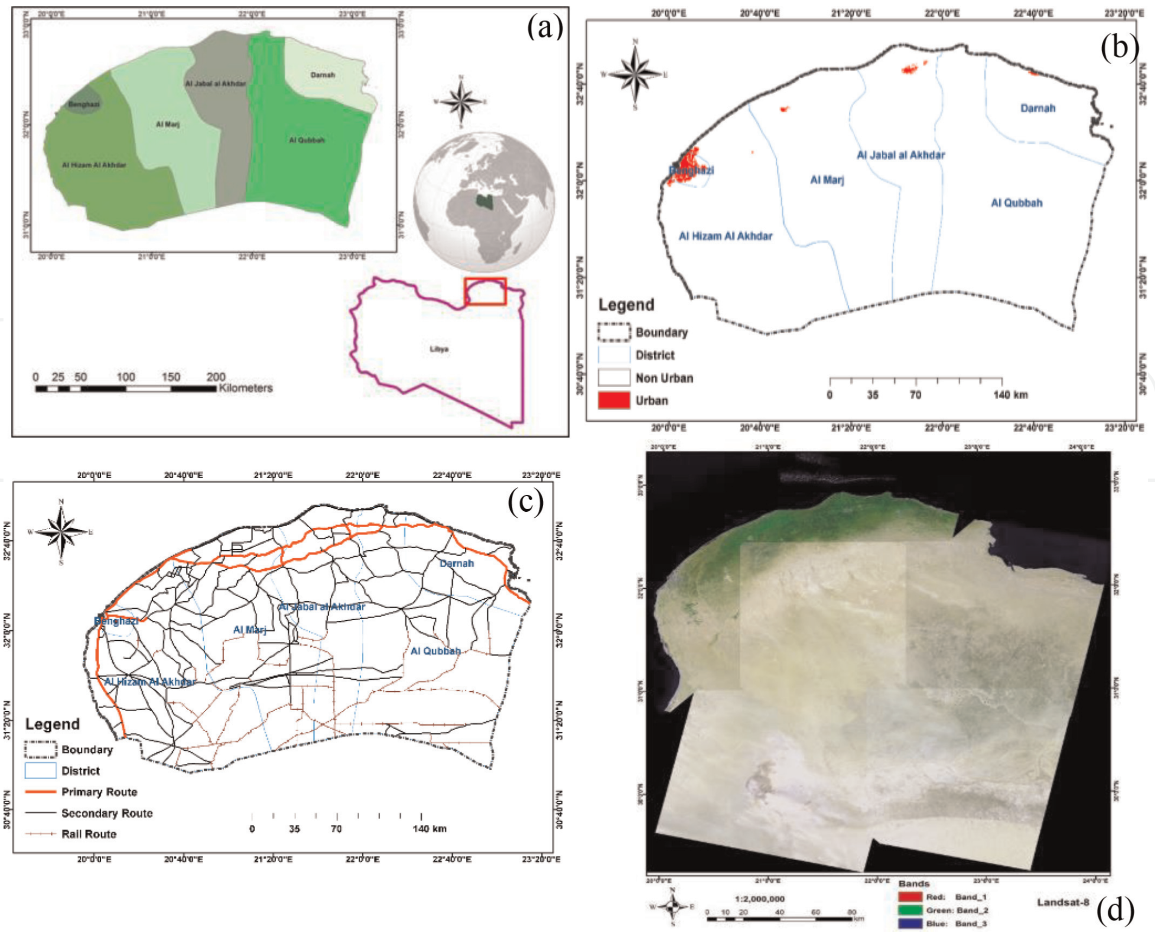


**Figure 1.**
*(a) Map of Libya with northern part highlighted, (b) the location of the urban area, (c) the road networks in the study area, and (d) mosaicked Landsat images.*

Al Hizam Al Akhdar (**Figure 1**). Libya is geographically bounded between 20°00′00″ E and 23°30′00″ E and 31°00′00″ N and 33°00′00″ N. The climate in Libya is categorized by hot and dry summers with high temperatures. The mean annual temperature in the coastal region ranges from 14.2°C (Shahat) to 21.0°C (Tripoli Airport) and at stations in the interior region (inland) between 21.3°C (Al Qaryat) and (Ghat) 23.4°C (1945–2009). Libya is one of the driest countries in the world with mean annual rainfall along the Libyan coast ranging between 140 and 550 mm and rarely exceeding 50 mm in the interior regions (1945–2010). December and January are the wettest months with 6 months (October–March) receiving 87.1% of the total annual precipitation. The majority of rainfall occurs in the winter season with the rainy season beginning in September-October and ends in March-April [21].

## 2.1 Data preparation

The data used in this study include Landsat satellite imagery acquired in the year 2017 with 15 m resolution panchromatic and 30 m resolution multispectral, Shuttle Radar Topography Mission (SRTM) digital elevation model (DEM) downloaded from USGS data archive with 30 m resolution, population density map obtained from GHSL with 250 m resolution, road network map from Diva-GIS, and MODIS satellite imagery from where the land surface temperature with 0.25° resolution was derived. Other data include rainfall data at 0.25°, net primary productivity (NPP) at 0.1°, NDVI at 0.1°, and air quality (CO, $NO_2$) at 0.25° resolution (**Table 1**). Details of the Landsat data are presented in **Table 2**. Seven set of images with overlapping areas were acquired between 4 February 2017 and 1 March 2017. In addition, the

| Data | Source | Resolution |
|---|---|---|
| Landsat satellite imagery | USGS | 30 m |
| DEM | USGS | 30 m |
| Population density | GHSL | 250 m |
| Road network | Diva GIS | / |
| Land surface temperature | MODIS | 0.25° |
| Rainfall | MODIS | 0.25° |
| Net primary productivity | MODIS | 0.1° |
| NDVI | MODIS | 0.1° |
| Air quality ($CO$, $NO_2$) | MODIS | 0.25° |

**Table 1.**
*Information of the datasets used in the research.*

| Image ID | Acquisition date | Raw | Path | Cloud cover (%) |
|---|---|---|---|---|
| Landsat 8 OLI 1 | 1 March 2017 | 38 | 182 | 0.77 |
| Landsat 8 OLI 2 | 13 February 2017 | 39 | 182 | 1.03 |
| Landsat 8 OLI 3 | 4 February 2017 | 38 | 183 | 0.00 |
| Landsat 8 OLI 4 | 4 February 2017 | 37 | 183 | 0.11 |
| Landsat 8 OLI 5 | 4 February 2017 | 39 | 183 | 0.13 |
| Landsat 8 OLI 6 | 19 February 2017 | 37 | 184 | 1.00 |
| Landsat 8 OLI 7 | 19 February 2017 | 38 | 184 | 0.00 |

**Table 2.**
*Information of the Landsat images.*

highest cloud cover was 1.03%, which does not pose a problem for land use information extraction from the study area. Since the images have overlapping areas, they were preprocessed and mosaicked to create one seamless image of the area for effective and efficient processing (**Figure 1d**).

### 2.2 Data preprocessing

Four preprocessing steps were performed on the Landsat satellite images: (i) Pan-sharpening using a fusion of the panchromatic and multispectral bands for the enhancement of the spatial resolution of multispectral band; (ii) atmospheric correction, which is applied to correct the atmospheric distortion by retrieving surface reflectance and engage topographic correction as well as adjacency effect correction; (iii) radiometric correction, which converts radiance values to the pure surface reflectance to enhance image capability and contrast; and (iv) mosaicking to create one seamless image coverage of the area for effective and efficient processing [22]. The MODIS source data was preprocessed using MODIS Conversion Tool Kit (MCTK). Note that the spatial resolution of the MODIS dataset varied according to the source. However, during the preprocessing, they were resampled to 30 m to match the DEM and Landsat resolutions.

### 2.3 Urban conditioning factor dataset

In this study, we considered 17 critical urban conditioning factors for selecting the most suitable city or cities for sustainable urban development. The factors are grouped into five main categories: (i) topography, (ii) land use and infrastructure, (iii) demography and climate, (iv) vegetation, and (v) air quality.

### 2.3.1 Topography

Topography is a very important consideration for urban development projects [23]. For this study, altitude and slope are the two main factors related to topography. Altitude is important for citing facility because it affects the living conditions as well as breathing behavior. The collected DEM shows that the study area is between −4 and 865 m above mean sea level (**Figure 2a**). The slope factor, which ranges from 0 to 14° (can be classified as almost flat), was also generated (**Figure 2b**). Such data is important when estimating cost. For example, any increase in slope will increase the cost of facility installation and maintenance since moving workers, transport vehicles, and machineries will be more difficult (i.e., up and down a slope). Low slope areas also may incur undesirable cost, in the instance of weather anomalies such as dust/sand storms.

### 2.3.2 Land use and infrastructure

Land use and infrastructure are also important considerations for urban projects. Land use information can show human activity patterns, whereas infrastructure can indicate development status in a particular city. The land use of the study area was derived from Landsat images and refined based on Google maps (**Figure 2c**). In this study we applied the SVM classifier, which was based on object-based image analysis (OBIA) using the ENVI 5.3 software. Training sites for the SVM were collected form all land use classes by stratified random method (i.e., at least 80 sample points for each class) [24]. The area contains five main land use types: (i) irrigated crops, (ii) vegetation, (iii) artificial areas, (iv) bare lands, and (v) waterbodies. Most parts of the study area were bare land (desert), which were predominantly located in the middle and southern parts of the study area. The northern part mostly comprised of irrigated crops and artificial areas, specifically man-made features and urban areas.

Road networks play an important role in the country's economy, serving the people by linking main cities to industrial and commercial sites. In this study, three types of roads, namely, main routes, secondary routes, and trail routes (**Figure 2d–f**), were considered as factors for city selection. The northern part of the city is supported by main routes (**Figure 2d**). These roads mainly link other cities to Benghazi, which support Benghazi city itself. Main routes span a significant number of kilometers within the study area. The study area also contains several kilometers of secondary routes (**Figure 2e**). Unlike main routes, secondary routes are found in most parts of the study area and in different cities including Benghazi. Secondary routes mainly support transportation of goods and are used for civil construction projects. Finally, trail routes support the rural areas, mainly for transportation of agricultural produce to the markets. The class of roads plays a vital role in selecting a city for development according to the available budget. Cities that can support more people will normally be prioritized for development projects.

Another important factor related to infrastructure is the percentage of built-up areas in a particular city. This is important because cities with many built-up areas indicate little or no space for new projects. On the contrary, cities with fewer built-up areas mean that they are more suitable for new developmental projects. The Normalized Difference Built-up Index (NDBI), which is a quantity of the intensity of urban area from satellite images, was used in this study [25]. The NDBI was initially established regarding the ratio of bands 4 and 5 of TM sensor. However, the NDBI can be adopted on Landsat-8 data or even any multispectral sensor data [26]. It basically extracts the urban areas where there is an upper reflectance in the short-wave infrared band associated to the near-infrared band. The accuracy of built-up areas extracted using NDBI is reported to be around 93% [27, 28]. We calculate the NDBI (Eq. (1)) based on the work in [27]:

$$NDBI = \frac{SWIR - NIR}{SWIR + NIR} \tag{1}$$

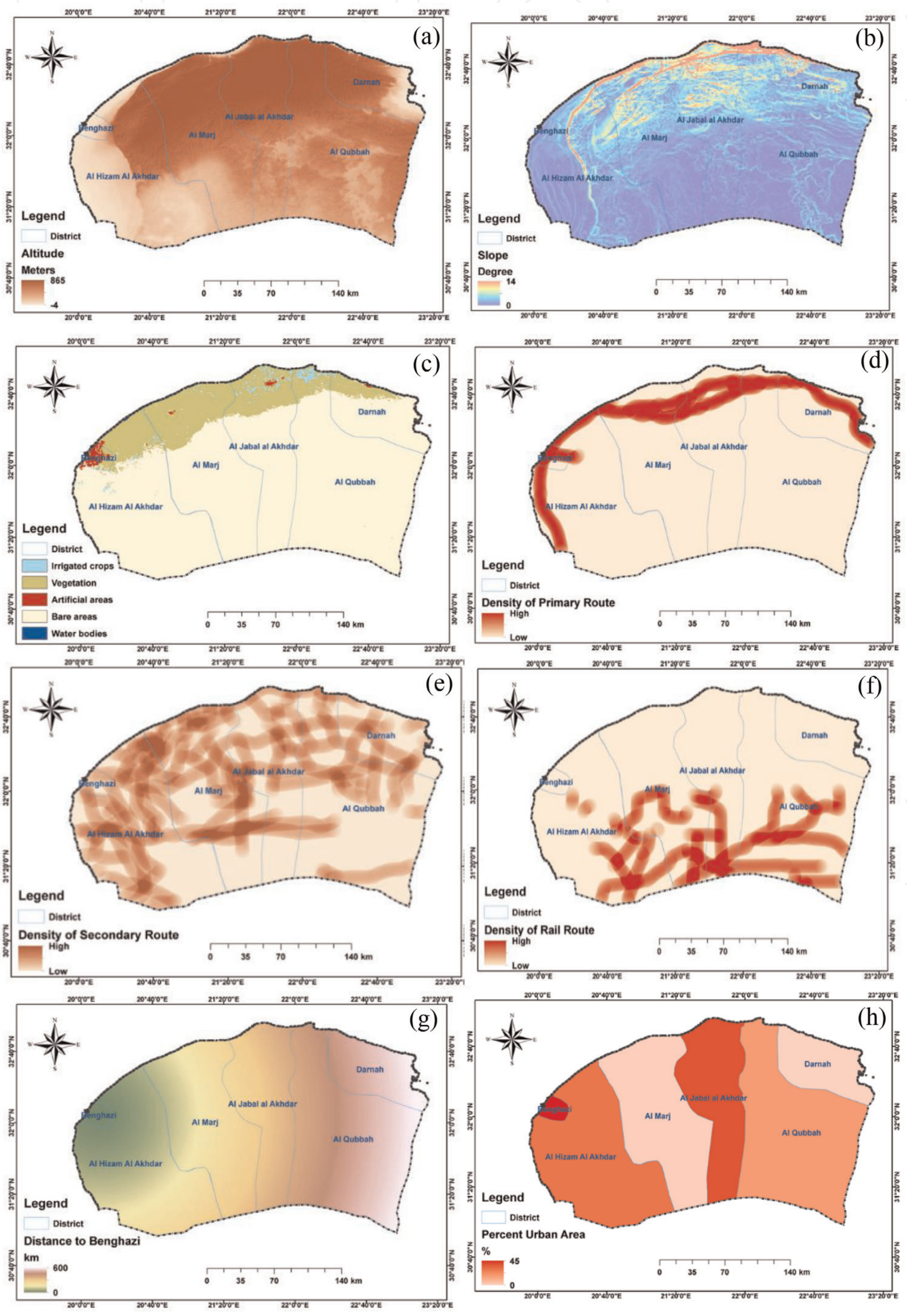

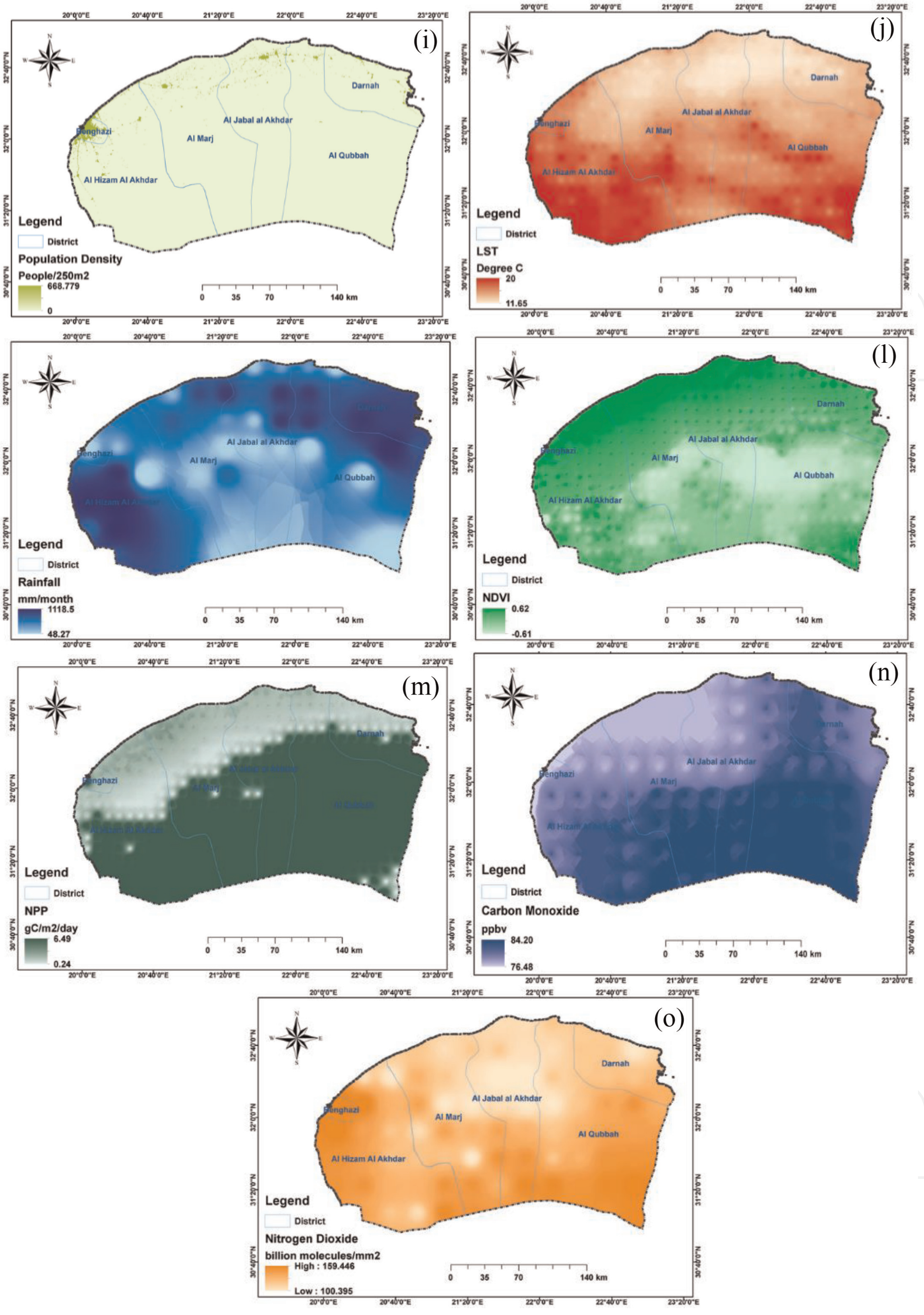


**Figure 2.**
*Elevation criteria: (a) altitude, (b) slope, (c) land use, (d) distance to the primary routes, (e) distance to the secondary routes, (f) distance to the trails, (g) distance to the Benghazi city, (h) percent of urban areas, (i) population density, (j) LST, (k) rainfall, (l) NDVI, (m) NPP product, (n) CO concentrations, (o) $NO_2$ concentrations.*

*SWIR* is the short-wave infrared band ranging from 1.57 to 1.65 $\mu m$. *NIR* is the near-infrared band in the range of 0.85–0.88 $\mu m$. **Figure 2h** shows the percentage of built-up areas calculated for each district considered in this work. The largest built-up area is found in Benghazi city (>45%). Some cities though, such as Al Marj and Darnah, have very small of built-up areas that are not detectable through satellite data.

Besides infrastructure factors, distance to the city is also a critical factor. Preferably, a city's location should be as near as possible to the capital or large cities such as Benghazi. This is because it facilitates ease of access to better business opportunities and education. Therefore, in this work, the distance to Benghazi city is one of the important parameters. Specifically, the desired distance to the city should range from 0 to 600 km (**Figure 2g**) so that cities such as Darnah and Al Qubbah (which are as far as 400 km away from Benghazi) are also covered.

#### *2.3.3 Demography and climate*

An increase in a city's population often leads to an increase in urbanization. Moreover, if the population increase is rapid, urbanization often happens randomly. This can be a major problem for most cities in a developing country. However, proper planning and effective decision-making can mitigate this problem. In this study, the population density (**Figure 2i**) was analyzed. The analysis results indicate that the northern part (mostly around Benghazi city) is most populated with a density of 669 people per 250 m cell of raster data.

Climate is a factor that also influences the selection of cities for developmental projects. Land surface temperature (LST) and rainfall are two factors considered in this work (**Figures 2j** and **3k**). The LST map shows that the southern part of the study area (mostly desert with no vegetation) has higher surface temperature compared to the northern parts. Another observation from the map reveals that Benghazi has slightly higher temperature than other urbanized areas. In arid regions, people often prefer to settle in areas with low temperature. The average day-night temperature ranges from 11° to 20° Centigrade. High temperatures are also observed in the west-southern part, whereas the lowest temperature is found in the northern part of Al Jabal Al Akhdar cities.

Rainfall, which is another climate factor, is also considered in deciding the location of settlement and development. This is because rainfall frequency and intensity affect the dryness of the cities, the local climate system, as well as agriculture activities. **Figure 2k** presents the rainfall intensity of the study area for year 2016 where minimum and maximum rainfall intensities were 48 and 1119 mm per month, respectively. The central part of the area has less amount of rainfall compared to other areas.

#### *2.3.4 Vegetation*

Normalized difference vegetation index (NDVI) is an indicator derived from remote sensing satellite data. It is mostly used to monitor vegetation cover over any area on the planet. It serves as a good indicator for vegetation cover of the study area. The presence of abundant vegetation is able to lower the local temperature as well as reduces the negative effects of noise and air pollutants. In the study area, the northern part has higher NDVI compared to the south (**Figure 2l**).

Larger amounts of vegetation can indicate higher vegetation productivity. Having higher vegetation productivity helps asses the net primary productivity (**Figure 2m**). Plant productivity plays a major role in the global carbon cycle by absorbing some of the carbon dioxide released through coal, oil, and other fossil-fuel burning. Large NPP values are found in the southern part of the study area.

### *2.3.5 Air quality*

Air quality directly affects the environment and consequently people's health. In this work, we have considered the CO and $NO_2$ (**Figure 2n** and **o**) air quality indicators. In 2016, higher CO and $NO_2$ levels were measured in the southern part of Benghazi. Benghazi city also recorded high levels of these gasses for the year under investigation. The air quality data was extracted from the MODIS source with a resolution of 0.25°. We utilized the ENVI 5.3 software to process the MODIS imagery. However, in order to prepare unprocessed MODIS satellite images for analysis, they must firstly be converted into ENVI format. This was done using the MODIS Conversion Tool Kit.

## 3. Modeling process

This section describes the modeling process, specifically the application of TOPSIS for scheduling and prioritizing the cities for urban development (**Figure 3**). First, a medium-resolution Landsat-8 satellite image from the study area was acquired and preprocessed. Then, the image was segmented using a multiresolution segmentation algorithm and classified into several classes using object-based image classification. The multiresolution algorithm has three main parameters, namely, scale, shape, and compactness. Since these parameters are data and application dependent, in this study, we had to select them empirically via trial and error. This meant that the best values were determined via visual examination of the segmentation results. After the segmentation process, several attributes were selected and used as class predictors in the classification algorithm. From the spectral attributes, the five bands of the Landsat-8 image were selected. For spatial attributes, shape index, roundness, compactness, and density were used [29, 30]. In the classification step, the support vector

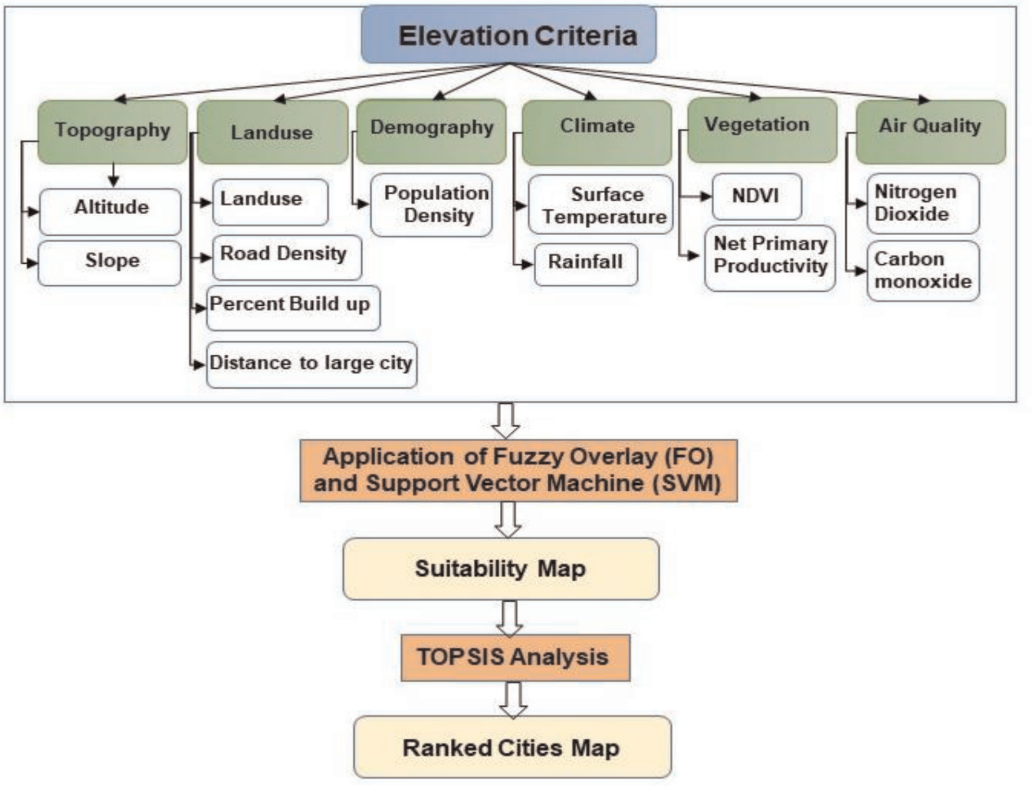


**Figure 3.**
*Flowchart of the methodology implemented in this study.*

machine (SVM) algorithm was used. Although the SVM is a relatively simple binary classifier, it has very good generalization capabilities if properly trained [31, 32].

Several other digital data such as DEM and population density were also obtained from various online sources. The factors used as described in the previous section are widely reported in the literature for selecting urban projects or relevant projects. Fuzzy overlay (FO) analysis was carried out to determine the importance of each parameter to achieving the goal of the study. The SVM classifier was further applied to refine the results obtained from the FO model. Finally, the cities were sorted according to their importance by applying the TOPSIS model on the results of the SVM.

### 3.1 Fuzzy overlay and TOPSIS models

Fuzzy overlay analysis is based on the fuzzy set theory that relies on membership relationship of events to define specific sets or classes [33]. Operationally, FO is similar to overlay analysis but differs in the reclassified values and results from the combination of multiple criteria. It involves problem definition, partitioning into sub-models and determining the significant layers. FO transforms the data to a common scale and defines the likelihood of the data belonging to a specific class, for example, slope values being transformed into the probability of fitting into the favorable suitability set based on a scale of 0 to 1, expressed in terms of membership [34]. Input raster are not weighted in FO since the transformed values indicate the possibility of membership rather than using ratio scale as with weighted overlay and weighted sum. The equation using fuzzy Gaussian function can be given as [35]

$$\mu(x) = e^{-f_i^{*}(x-f_2)^2} \tag{2}$$

The inputs $f_i$ and $f_2$ are the spread and the midpoint, respectively. Midpoint can be a user-defined value with a fuzzy membership of 1. The default is the midpoint of the range of values of the input raster. Spread defines the membership of the Gaussian function. It generally ranges from 0.01 to 1. Increasing the spread causes the fuzzy membership curve to become steeper. Fuzzy overlay analysis quantifies the possibilities of each cell or location to a specified set based on membership value.

As previously mentioned, the results of FO are refined using the SVM, which develops a linear regression between suitability status and criteria factors. SVM aims to determine an optimal separating hyperplane (maximizing the margin width) between two classes in feature space [36]. The training points near the hyperplane are called support vectors and are utilized for classification once the decision line/surface is obtained. The separating hyperplane is found as follows:

$$y_i(w \times x_i + b) \geq 1 - \varepsilon_i \tag{3}$$

where $w$ is the cofficienct vector that defines the hyperplane orientation in the feature space, $b$ is the offset of the hyperplane from the origin, and $\varepsilon_i$ is the positive slack variables. The optimal hyperplane is found by solving the following optimization problem [36, 37]:

$$\begin{gathered} \text{Minimize} \sum_{i=1}^{n} \alpha_i - \frac{1}{2} \sum_{i=1}^{n} \sum_{j=1}^{n} \alpha_i \alpha_j y_i y_j \left(x_i x_j\right) \\ \textit{subject} \sum_{i=1}^{n} \alpha_i y_i = 0,\ 0 \leq \alpha_i \leq C \end{gathered} \tag{4}$$

where $\alpha_i$ is the Lagrange multiplier and $C$ is the penalty for data classification. The following decision function is applied as follows:

$$g(x) = sign \tag{5}$$

Developed in [38–40], TOPSIS is a multi-criteria decision tool based on the intuition that a selected alternative has the shortest possible geometric distance from the PIS. In other words, the alternative has the longest geometric distance from the NIS [41]. The analysis compares a set of alternatives by assigning weightage to each criterion to compute the geometric distance between possible alternatives to determine the ideal alternative based on the assumption that the criteria uniformly increases or decreases. TOPSIS allows trade-offs between criteria; a poor result in one criterion can be compensated by a good result in another criterion. TOPSIS provides a more realistic model than non-compensatory methods by including or excluding alternative solutions using hard cutoffs. Consider $X_{ij}$ as the inputs for matrix of priorities where there are $i = 1, \ldots, m$ alternatives and $j = 1, \ldots, n$ criteria. There are six steps associated with the implementation of TOPSIS as follows [42]:

Step 1: Construct the normalized decision matrix calculated using Eq. (6):

$$r_{ij} = \frac{x_{ij}}{\sqrt{\sum_{i=1}^{m}\sum_{j=1}^{n} x_{ij}^2}} \tag{6}$$

Step 2: Construct the weighted normalized decision matrix using Eq. (7):

$$v_{ij} = w_i r_{ij}, i = 1, \ldots, mj = 1, \ldots, n \tag{7}$$

Step 3: The positive and negative ideal solutions are determined by

$$\begin{aligned} A^+ &= \{v_1^+, \ldots, v_n^+\}, \text{where } v_j^+ = \{\max(v_{ij}) if\ j \in J; \min(v_{ij}) if\ j \in J'\} \\ A^- &= \{v_1^-, \ldots, v_n^-\}, \text{where } v_j^* = \{\min(v_{ij}) if\ j \in J; \min(v_{ij}) if\ j \in J'\} \end{aligned} \tag{8}$$

Step 4: Calculation of separation (positive and negative) measurement using Euclidean distance. Eq. (9) is used to calculate the distance.

$$S_i^+ = \sqrt{\sum_{j=1}^{n}\left(v_j^+ - v_{ij}\right)^2}, S_i^- = \sqrt{\sum_{j=1}^{n}\left(v_j^- - v_{ij}\right)^2}, \ i = 1, \ldots, m \tag{9}$$

Step 5: Closeness to the ideal solution is calculated using Eq. (10):

$$C_i^+ = \frac{S_i^-}{S_i^- + S_i^+}, 0 < C_I^+ < 1, i = 1, \ldots, m \tag{10}$$

Step 6: Ranking alternatives based on closeness to the ideal solution. TOPSIS has been used in different circumstances (e.g., individual and grouping). By applying the TOPSIS model using the results of the FO as input, the cities were sorted according to their importance for proposed urban development projects.

## 4. Results and discussion

According to [43], the most contributing factors to urban suitability are topography, land use and infrastructure, vegetation, demography and climate, and air quality. Therefore, these factors should be thoroughly analyzed to discover the most (and the least) suitable area for urbanization. Hence, in this work, 17 detailed factors were analyzed in order to rank each's importance (via weight assignment) for the selection of a city (or cities) for sustainable urban development. Subsequently, a suitability map was generated based on the FO (**Figure 4a**) method. A continuous scale was used for suitability weightage, which ranges from 0 (less suitable) to 1 (highly suitable). From the generated map, areas indicated as most suitable are located in the northern parts, especially the areas surrounding Benghazi and the northern parts of Al Marj and Al Jabal Al Akhdar. Sole reliance on the generated map, however, does not help much in deciding city development prioritization. As a result, the map was further refined to make it much more distinct for decision-makers. To do this, the map was firstly reclassified into three categorical classes: (i) not suitable, (ii) less suitable, and (iii) highly suitable. This was done using the natural break classification method (**Figure 4b**) where several samples were selected from the not suitable and highly suitable areas (results of FO) to generate training and testing data. These datasets were then used to train a SVM to classify between the two classes. **Table 3** presents the estimated factors and their coefficients. The result indicates that land use, distance to primary route,

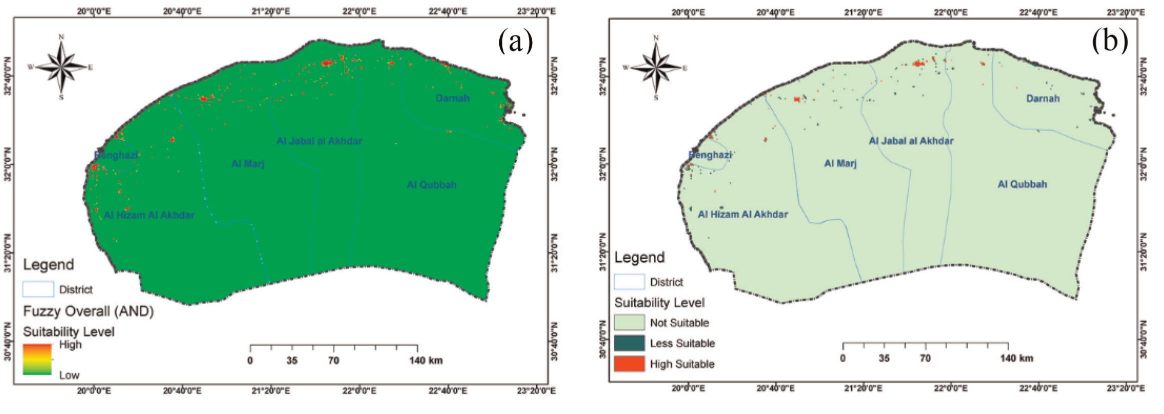


**Figure 4.**
*Results of fuzzy overlay in (a) continuous scale and (b) categorical format.*

| Evaluation criteria | SVM weight | Criteria code |
|---|---|---|
| Land use | −0.36 | C12 |
| Percent built-up area | 0.97 | C1 |
| NDVI | 2.15 | C10 |
| Altitude | 0.60 | C15 |
| Slope | 0.96 | C7 |
| Distance to primary route | −2.35 | C4 |
| Distance to secondary route | 0.74 | C6 |
| Distance to trail lines | 0.27 | C8 |
| Distance to capital city | −0.62 | C13 |
| Population density | 4.88 | C3 |
| Rainfall | −1.17 | C5 |
| LST | 0.23 | C11 |
| NPP | −0.10 | C2 |
| Carbon monoxide | 1.23 | C14 |
| Nitrogen dioxide | −1.18 | C9 |

**Table 3.**
*List of criteria, estimated coefficient, and their code.*

distance to capital city, rainfall, NPP, and $NO_2$ have negative effects on the suitability level of the selection process. The remaining factors have positive effects. Among the positive factors, population density has the highest effects on the selection process.

Based on the estimated coefficients, the suitability map in **Figure 5** was produced. It can be seen that the map reflects the same thing as in the previous suitability map. However, it is clearly more informative for decision-makers. Based on this, the cities were ranked according to their importance using TOPSIS method.

### 4.1 TOPSIS analysis

**Table 4** presents the positive ideal, negative ideal, closeness coefficient, and TOPSIS rank for each of the cities being analyzed. According to the closeness coefficients, the ranking order for the cities is as follows:

1. Benghazi
2. Al Jabal Al Akhdar
3. Al Marj
4. Darnah
5. Al Hizam Al Akhdar
6. Al Qubbah

The ranking results were then used to generate a map for final decision-making (**Figure 6**). Cities with green and light green colors are suggested to be prioritized first for development. More details about the TOPSIS analysis can be found in the Appendices.

Based on the results, the importance of each group of factors was evaluated (**Figure 7**). The bar chart shows the importance of the standardized factor weights

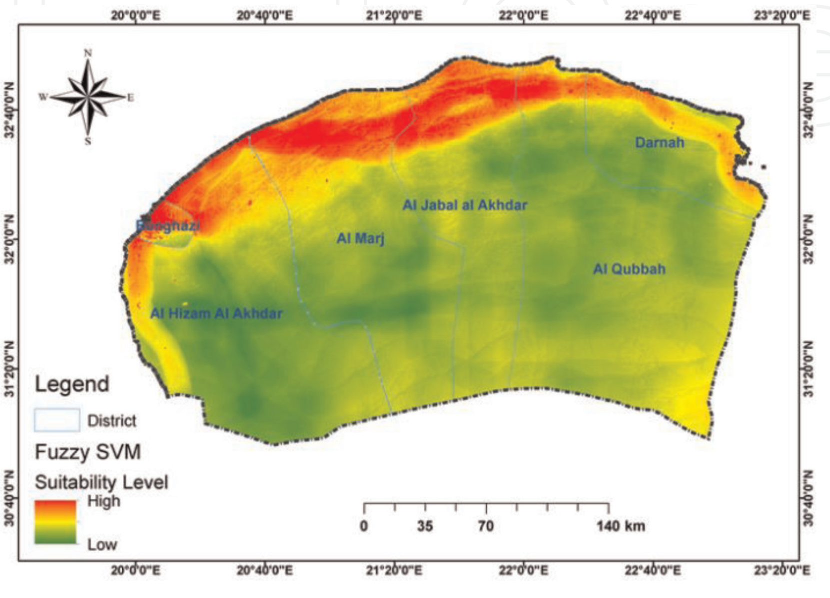


**Figure 5.**
*FO after refinement with SVM.*

| City | A+ | A− | Closeness coefficient | TOPSIS rank |
|---|---|---|---|---|
| Darnah | 2.58 | 1.41 | 0.35 | 4 |
| Al Jabal Al Akhdar | 2.05 | 1.74 | 0.46 | 2 |
| Benghazi | 0.98 | 3.40 | 0.77 | 1 |
| Al Marj | 2.23 | 1.57 | 0.41 | 3 |
| Al Qubbah | 3.13 | 1.08 | 0.25 | 6 |
| Al Hizam Al Akhdar | 2.69 | 1.29 | 0.32 | 5 |

**Table 4.**
*Ranking of cities on the basis of importance for urban development.*

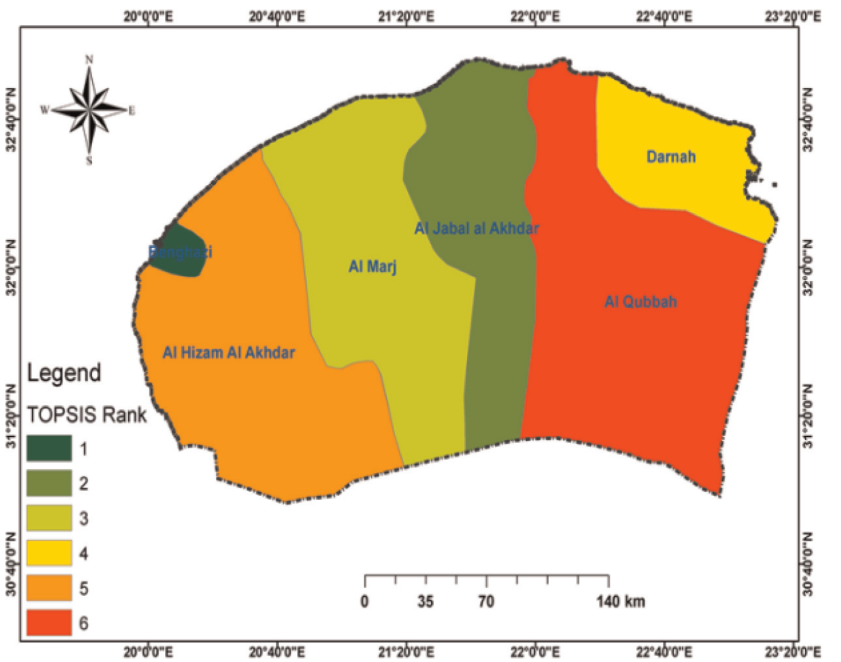


**Figure 6.**
*The map showing the cities' ranks based on TOPSIS.*

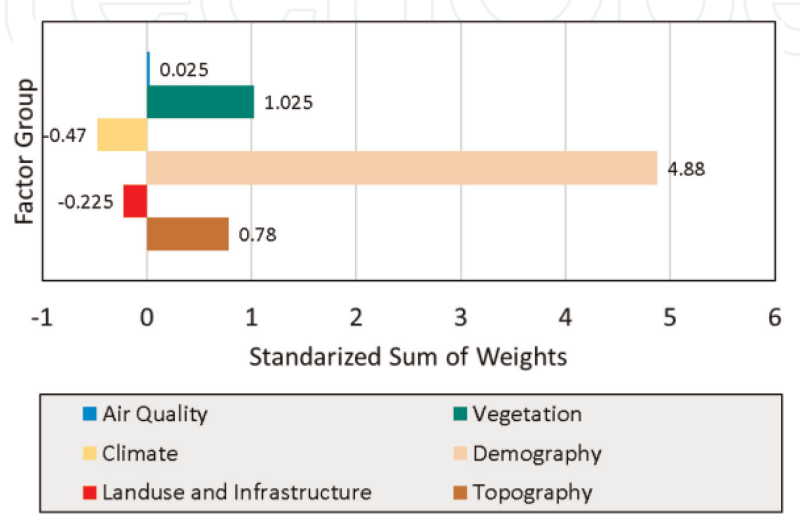


**Figure 7.**
*Importance degree of factor groups.*

in each group. Demography and vegetation are the two most influential factors with positive contribution, followed by vegetation and topography. The other factors have negative contribution.

### 4.2 Accuracy assessment

Recall that the refined suitability map was recategorized into the three classes of “not suitable,” “less suitable,” and “highly suitable,” These classes reflect the degree of urban development suitability in the study area. The categorized suitability map can be validated accurately through each class. The continuous refined is suitability map ranging from 0 to 1. The most suitable areas that range from 0.751 to 1 fall into high suitable class, while the moderate suitable areas for urban development were extracted from 0.401 to 0.751 from the continuous refined suitability map.

| Accuracy metric | Value |
|---|---|
| Correctly classified instances | 1178 (78.5%) |
| Incorrectly classified instances | 322 (21.4%) |
| Kappa statistic | 0.67 |

**Table 5.**
*Overall accuracy assessment of SVM modeling.*

| Class | ROC area | PRC area |
|---|---|---|
| Not suitable | 0.934 | 0.884 |
| Less suitable | 0.799 | 0.60 |
| High suitable | 0.852 | 0.673 |
| Average | 0.861 | 0.719 |

**Table 6.**
*Accuracy assessment of SVM modeling based on ROC.*

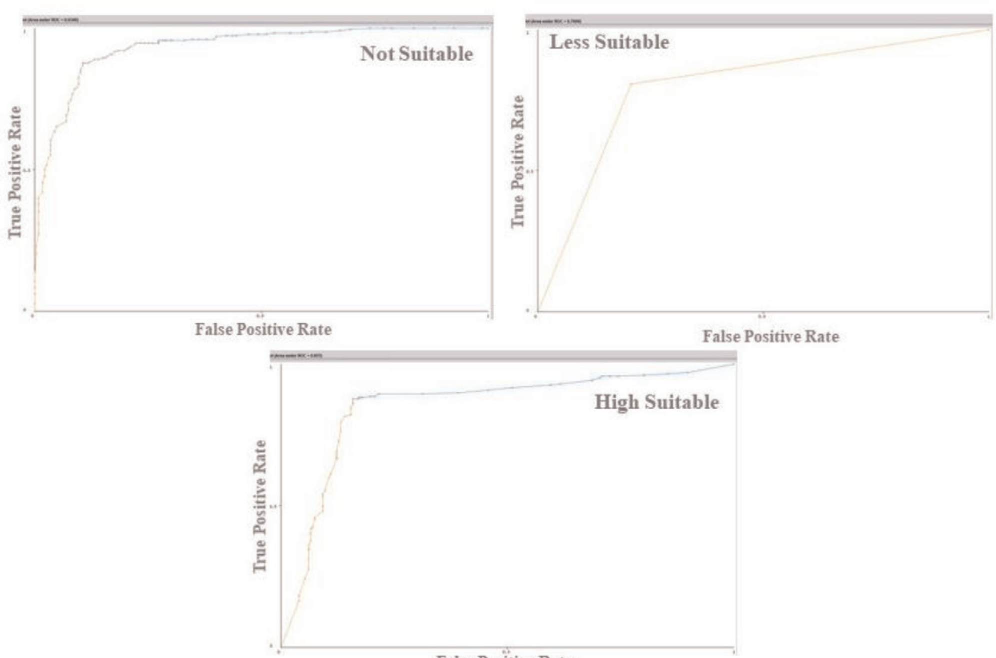


**Figure 8.**
*AUC for the SVM.*

Consequently, the least feasible areas were classified out of 0.001 to 0.40. The categorized suitability map was then validated based on the same randomly selected samples (**Table 5**). The SVM model accurately classified 1178 samples, which is about 78.5% of the total samples tested, which produced kappa index of 0.67. The kappa index is calculated using Eq. (11) [44]:

$$K = \frac{P_C - P_{exp}}{1 - P_{exp}} \tag{11}$$

where $P_c$ is the proportion of number of pixels that are correctly classified and is calculated as $\frac{(TP+TN)}{totalnumberofpixels}$. $P_{exp}$ is the expected agreements and is calculated as $\frac{(TP+FN)(TP+FP)+(FP+TN)(FN+TN)}{\sqrt{(totalnumberoftrainingpixels)}}$. Since both the "not suitable" and "highly suitable" classes are important for the final mapping and ranking of the cities, we also evaluated the results using the area under the ROC curve (**Table 6**), which gives an indication of the global statistical accuracy of the models. If the AUC, which varies from 0.5 to 1, increases toward 1, it indicates better performance prediction [45]. The highest and lowest success rates are 0.939 and 0.793, while the highest and lowest prediction rates are 0.884 and 0.673, respectively (**Figure 8**).

## 5. Conclusion

An automated geospatial solution for selecting and ranking cities in Libya for urban development is proposed in this chapter. The suitability map showed that most areas indicated to be suitable are in the northern part of Libya. The results indicate that land use, distance to primary route, distance to large city, rainfall, NPP, and $NO_2$ have negative effects on the level of suitability for the selection process, whereas the other factors have positive effects with population density taking the lead. It is revealed that SVM model accurately classifies 1178 samples, about 78.5% of the total samples tested which produced kappa statistic of 0.67. The high-priority city was selected as Benghazi that is followed by Al Jabal Al Akhdar. The results suggest that demography and vegetation are the two most influential factors contributing to the selection of city for development in Libya. This study is limited to analysis of six cities; the procedure developed through this study can be extended to other cities. It is of the opinion that evaluated criteria can be adjusted according to the environment and the current development of the cities.

## A. Appendix

TOPSIS 1

| City | Percent urban | NPP | Population | Primary route | Rainfall | Secondary route | Slope | Trail route | NO | NDVI | LST | land cover | Distance to Benghazi | CO | Altitude |
|---|---|---|---|---|---|---|---|---|---|---|---|---|---|---|---|
| | C1 | C2 | C3 | C4 | C5 | C6 | C7 | C8 | C9 | C10 | C11 | C12 | C13 | C14 | C15 |
| Darnah | 0.37 | 3.68 | 131333.00 | 142935.00 | 680.50 | 356539.00 | 0.86 | 0.00 | 118.32 | −0.42 | 14.46 | 200 | 139404.00 | 81.09 | 226.11 |
| Al Jabal Al Akhdar | 0.49 | 4.20 | 224171.00 | 196505.00 | 422.65 | 696167.00 | 0.82 | 221496.00 | 117.11 | −0.34 | 15.11 | 200 | 162514.00 | 79.77 | 341.61 |
| Benghazi | 44.77 | 2.18 | 571466.00 | 52346.60 | 370.37 | 41068.40 | 0.36 | 27.63 | 148.66 | −0.10 | 17.19 | 30 | 541.96 | 78.36 | 55.55 |
| Al Marj | 0.11 | 4.12 | 202732.00 | 188407.00 | 409.90 | 1328530.00 | 0.62 | 395212.00 | 120.24 | −0.30 | 15.86 | 200 | 147881.00 | 80.26 | 261.23 |
| Al Qubbah | 0.00 | 5.83 | 47112.30 | 75610.90 | 461.25 | 906233.00 | 0.36 | 555787.00 | 127.56 | −0.52 | 16.51 | 200 | 441023.00 | 82.69 | 209.68 |
| Al Hizam Al Akhdar | 0.28 | 4.31 | 164855.00 | 170954.00 | 598.51 | 1449880.00 | 0.39 | 346141.00 | 127.79 | −0.41 | 17.47 | 200 | 110122.00 | 80.76 | 122.89 |
| Criteria sign range | −1 | 1 | 1 | 1 | 1 | 1 | −1 | 1 | −1 | 1 | −1 | −1 | −1 | −1 | −1 |
| W(Lambda) | −0.36 | 0.98 | 2.15 | 0.60 | 0.96 | −2.35 | 0.74 | 0.27 | −0.62 | 4.88 | −1.17 | 0.23 | −0.10 | 1.23 | −1.18 |
| Ideal | 0.00 | 5.83 | 571466.00 | 196505.00 | 680.50 | 1449880.00 | 0.36 | 555787.00 | 117.11 | −0.10 | 14.46 | 30.00 | 541.96 | 78.36 | 55.55 |
| The worst | 44.77 | 2.18 | 47112.30 | 52346.60 | 370.37 | 41068.40 | 0.86 | 0.00 | 148.66 | −0.52 | 17.47 | 200.00 | 441023.00 | 82.69 | 341.61 |

TOPSIS 2

| | C1 | C2 | C3 | C4 | C5 | C6 | C7 | C8 | C9 | C10 | C11 | C12 | C13 | C14 | C15 |
|---|---|---|---|---|---|---|---|---|---|---|---|---|---|---|---|
| | 44.40 | 3.68 | 131333.00 | 142935.00 | 680.50 | 356539.00 | 0.00 | 0.00 | 30.35 | −0.42 | 3.00 | 0.00 | 301619.00 | 1.60 | 115.49 |
| | 44.28 | 4.20 | 224171.00 | 196505.00 | 422.65 | 696167.00 | 0.04 | 221496.00 | 31.56 | −0.34 | 2.35 | 0.00 | 278509.00 | 2.92 | 0.00 |
| N= | 0.00 | 2.18 | 571466.00 | 52346.60 | 370.37 | 41068.40 | 0.50 | 27.63 | 0.00 | −0.10 | 0.28 | 170.00 | 440481.04 | 4.33 | 286.06 |
| | 44.66 | 4.12 | 202732.00 | 188407.00 | 409.90 | 1328530.00 | 0.25 | 395212.00 | 28.42 | −0.30 | 1.60 | 0.00 | 293142.00 | 2.43 | 80.38 |
| | 44.77 | 5.83 | 47112.30 | 75610.90 | 461.25 | 906233.00 | 0.50 | 555787.00 | 21.11 | −0.52 | 0.95 | 0.00 | 0.00 | 0.00 | 131.93 |
| | 44.49 | 4.31 | 164855.00 | 170954.00 | 598.51 | 1449880.00 | 0.48 | 346141.00 | 20.87 | −0.41 | 0.00 | 0.00 | 330901.00 | 1.93 | 218.72 |
| Normal | 99.55 | 10.3 | 681594.73 | 363626.55 | 1232.02 | 2302576.25 | 0.88 | 796219.68 | 60.05 | 0.90 | 4.25 | 170 | 746988.97 | 6.28 | 408.49 |

TOPSIS 3

| C1 | C2 | C3 | C4 | C5 | C6 | C7 | C8 | C9 | C10 | C11 | C12 | C13 | C14 | C15 |
|---|---|---|---|---|---|---|---|---|---|---|---|---|---|---|
| 0.445 | 0.36 | 0.192 | 0.393 | 0.552 | 0.154 | 0 | 0 | 0.505 | −0.47 | 0.71 | 0 | 0.403 | 0.25 | 0.282 |
| 0.444 | 0.41 | 0.328 | 0.540 | 0.343 | 0.302 | 0.05 | 0.278 | 0.526 | −0.37 | 0.55 | 0 | 0.372 | 0.46 | 0 |
| 0 | 0.21 | 0.838 | 0.143 | 0.300 | 0.017 | 0.562 | 0 | 0 | −0.11 | 0.07 | 1 | 0.589 | 0.69 | 0.700 |
| 0.448 | 0.4 | 0.297 | 0.518 | 0.332 | 0.576 | 0.278 | 0.496 | 0.473 | −0.33 | 0.38 | 0 | 0.392 | 0.39 | 0.196 |
| 0.449 | 0.57 | 0.069 | 0.207 | 0.374 | 0.393 | 0.563 | 0.698 | 0.352 | −0.57 | 0.22 | 0 | 0 | 0 | 0.322 |
| 0.446 | 0.42 | 0.241 | 0.470 | 0.485 | 0.629 | 0.537 | 0.434 | 0.348 | −0.45 | 0 | 0 | 0.442 | 0.31 | 0.535 |

## TOPSIS 4

| | C1 | C2 | C3 | C4 | C5 | C6 | C7 | C8 | C9 | C10 | C11 | C12 | C13 | C14 | C15 |
|---|---|---|---|---|---|---|---|---|---|---|---|---|---|---|---|
| | −0.164 | 0.35 | 0.415 | 0.236 | 0.533 | −0.364 | 0 | 0 | −0.318 | −2.28 | −0.83 | 0 | −0.044 | 0.31 | −0.333 |
| | −0.163 | 0.4 | 0.709 | 0.325 | 0.331 | −0.711 | 0.037 | 0.075 | −0.331 | −1.8 | −0.65 | 0 | −0.040 | 0.57 | 0 |
| | 0 | 0.21 | 1.808 | 0.086 | 0.290 | −0.041 | 0.417 | 0 | 0 | −0.52 | −0.08 | 0.234 | −0.064 | 0.85 | −0.826 |
| | −0.165 | 0.39 | 0.641 | 0.311 | 0.321 | −1.356 | 0.206 | 0.134 | −0.298 | −1.62 | −0.44 | 0 | −0.043 | 0.48 | −0.232 |
| | −0.165 | 0.56 | 0.149 | 0.125 | 0.361 | −0.925 | 0.418 | 0.189 | −0.221 | −2.78 | −0.26 | 0 | 0 | 0 | −0.381 |
| | −0.164 | 0.41 | 0.521 | 0.283 | 0.468 | −1.480 | 0.398 | 0.118 | −0.219 | −2.18 | 0 | 0 | −0.048 | 0.38 | −0.632 |
| Ideal | 0.00 | 0.56 | 1.81 | 0.33 | 0.53 | −0.04 | 0.42 | 0.19 | 0.00 | −0.52 | 0.00 | 0.23 | 0.00 | 0.85 | 0.00 |
| The worst | −0.17 | 0.21 | 0.15 | 0.09 | 0.29 | −1.48 | 0.00 | 0.00 | −0.33 | −2.78 | −0.83 | 0.00 | −0.06 | 0.00 | −0.83 |

## TOPSIS 5

| C1 | C2 | C3 | C4 | C5 | C6 | C7 | C8 | C9 | C10 | C11 | C12 | C13 | C14 | C15 |
|---|---|---|---|---|---|---|---|---|---|---|---|---|---|---|
| 0.16 | 0.20 | 1.39 | 0.09 | 0.00 | 0.32 | 0.42 | 0.19 | 0.32 | 1.76 | 0.83 | 0.23 | 0.04 | 0.54 | 0.33 |
| 0.16 | 0.16 | 1.10 | 0.00 | 0.20 | 0.67 | 0.38 | 0.11 | 0.33 | 1.28 | 0.65 | 0.23 | 0.04 | 0.28 | 0.00 |
| 0.00 | 0.35 | 0.00 | 0.24 | 0.24 | 0.00 | 0.00 | 0.19 | 0.00 | 0.00 | 0.08 | 0.00 | 0.06 | 0.00 | 0.83 |
| 0.17 | 0.16 | 1.17 | 0.01 | 0.21 | 1.32 | 0.21 | 0.05 | 0.30 | 1.10 | 0.44 | 0.23 | 0.04 | 0.37 | 0.23 |
| 0.17 | 0.00 | 1.66 | 0.20 | 0.17 | 0.88 | 0.00 | 0.00 | 0.22 | 2.26 | 0.26 | 0.23 | 0.00 | 0.85 | 0.38 |
| 0.16 | 0.15 | 1.29 | 0.04 | 0.06 | 1.44 | 0.02 | 0.07 | 0.22 | 1.66 | 0.00 | 0.23 | 0.05 | 0.47 | 0.63 |

## Author details

Bahareh Kalantar[1]*, Husam A.H. Al-najjar[2], Hossein Mojaddadi Rizeei[2], Maruwan S.A.B. Amazeeq[3], Mohammed Oludare Idrees[3], Alfian Abdul Halin[4] and Shattri Mansor[3]

1 RIKEN Center for Advanced Intelligence Project, Goal-Oriented Technology Research Group, Disaster Resilience Science Team, Tokyo, Japan

2 Centre for Advanced Modelling and Geospatial Information Systems (CAMGIS), Faculty of Engineering and IT, University of Technology Sydney, NSW, Australia

3 Department of Civil Engineering, Faculty of Engineering, Universiti Putra Malaysia, Serdang, Selangor, Malaysia

4 Department of Multimedia, Faculty of Computer Science and Information Technology, Universiti Putra Malaysia, Serdang, Selangor, Malaysia

*Address all correspondence to: bahareh.kalantar@riken.jp

## References


[1] Juan YK, Roper KO, Castro-Lacouture D, Ha Kim J. Optimal decision making on urban renewal projects. Management Decision. 2010; **48**(2):207-224

[2] Coutinho-Rodrigues J, Simão A, Antunes CH. A GIS-based multicriteria spatial decision support system for planning urban infrastructures. Decision Support Systems. 2011;**51**(3): 720-726

[3] Mukherjee AB, Krishna AP, Patel N. Application of remote sensing technology, GIS and AHP-TOPSIS model to quantify urban landscape vulnerability to land use transformation. In: Information and Communication Technology for Sustainable Development. Singapore: Springer; 2018. pp. 31-40

[4] Donnay JP, Barnsley MJ, Longley PA, editors. Remote Sensing and Urban Analysis. London: Taylor and Francis; 2001. pp. 3-18

[5] Harris PM, Ventura SJ. The integration of geographic data with remotely sensed imagery to improve classification in an urban area. Photogrammetric Engineering and Remote Sensing. 1995;**61**(8):993-998

[6] Gandibleux X, editor. Multiple Criteria Optimization: State of the Art Annotated Bibliographic Surveys. Springer Science & Business Media; 2006;**52**

[7] Vafaeipour M, Zolfani SH, Varzandeh MHM, Derakhti A, Eshkalag MK. Assessment of regions priority for implementation of solar projects in Iran: New application of a hybrid multi-criteria decision making approach. Energy Conversion and Management. 2014;**86**:653-663

[8] Wang YJ. A fuzzy multi-criteria decision-making model based on simple additive weighting method and relative preference relation. Applied Soft Computing. 2015;**30**:412-420

[9] Mosadeghi R, Warnken J, Tomlinson R, Mirfenderesk H. Comparison of Fuzzy-AHP and AHP in a spatial multi-criteria decision making model for urban land-use planning. Computers, Environment and Urban Systems. 2015; **49**:54-65

[10] Abidin MZ, Rusli R, Shariff AM. Technique for Order Performance by Similarity to Ideal Solution (TOPSIS)-entropy methodology for inherent safety design decision making tool. Procedia Engineering. 2016;**148**: 1043-1050

[11] Zarghami M, Szidarovszky F, Ardakanian R. A fuzzy-stochastic OWA model for robust multi-criteria decision making. Fuzzy Optimization and Decision Making. 2008;**7**(1):1-15

[12] Zhang K, Achari G. Uncertainty propagation in environmental decision making using random sets. Procedia Environmental Sciences. 2010; **2**:576-584

[13] Mosadeghi R, Warnken J, Tomlinson R, Mirfenderesk H. Uncertainty analysis in the application of multi-criteria decision-making methods in Australian strategic environmental decisions. Journal of Environmental Planning and Management. 2013;**56**(8):1097-1124

[14] Montgomery B, Dragićević S, Dujmović J, Schmidt M. A GIS-based Logic Scoring of Preference method for evaluation of land capability and suitability for agriculture. Computers and Electronics in Agriculture. 2016; **124**:340-353

[15] Yoon K, Hwang CL. Manufacturing plant location analysis by multiple

attribute decision making: Part I —Single-plant strategy. International Journal of Production Research. 1985; **23**(2):345-359

[16] Awasthi A, Chauhan SS, Omrani H. Application of fuzzy TOPSIS in evaluating sustainable transportation systems. Expert Systems with Applications. 2011;**38**:12270-12280

[17] Uysal F, Tosun Ö. Fuzzy TOPSIS-based computerized maintenance management system selection. Journal of Manufacturing Technology Management. 2012;**23**(2):212-228

[18] Momeni M, Fathi MR, Zarchi MK, Azizollahi S. A fuzzy TOPSIS-based approach to maintenance strategy selection: A case study. Middle-East Journal of Scientific Research. 2011; **8**(3):699-706

[19] Baysal ME, Kaya İ, Kahraman C, Sarucan A, Engin O. A two phased fuzzy methodology for selection among municipal projects. Technological and Economic Development of Economy. 2015;**21**(3):405-422

[20] Shelton J, Medina M. Integrated multiple-criteria decision-making method to prioritize transportation projects. Transportation Research Record: Journal of the Transportation Research Board. 2010;**2174**:51-57

[21] Ageena IS. Trends and patterns in the climate of Libya. Thesis submitted in accordance with the requirements of the University of Liverpool for the degree of Doctor of Philosophy. 2013

[22] Mojaddadi Rizeei H, Pradhan B, Saharkhiz MA. Urban object extraction using Dempster Shafer feature-based image analysis from worldview-3 satellite imagery. International Journal of Remote Sensing. 2019;**40**(3):1092-1119

[23] Kia MB, Pirasteh S, Pradhan B, Mahmud AR, Sulaiman WNA, Moradi A. An artificial neural network model for flood simulation using GIS: Johor River Basin, Malaysia. Environmental Earth Sciences. 2012; **67**(1):251-264

[24] Aal-shamkhi AD, Mojaddadi H, Pradhan B, Abdullahi S. Extraction and modeling of urban sprawl development in Karbala City using VHR satellite imagery. In: Spatial Modeling and Assessment of Urban Form. Cham: Springer; 2017. pp. 281-296

[25] Bhatti SS, Tripathi NK. Built-up area extraction using Landsat 8 OLI imagery. GIScience & Remote Sensing. 2014; **51**(4):445-467. DOI: 10.1080/15481603.2014.939539

[26] Miscellaneous Indices Background. Normalized Difference Built-Up Index (NDBI). Harris Geospatial Solutions. URL: Available from: http://www.harrisgeospatial.com/docs/BackgroundOtherIndices.html [Accessed: 27 January 2016]

[27] Zha Y, Gao J, Ni S. Use of normalized difference built-up index in automatically mapping urban areas from TM imagery. International Journal of Remote Sensing. 2003;**24**(3):583-594

[28] Yang L, Xian G, Klaver JM, Deal B. Urban land-cover change detection through sub-pixel imperviousness mapping using remotely sensed data. Photogrammetric Engineering & Remote Sensing. 2003;**69**(9): 1003-1010. DOI: 10.14358/PERS.69.9.1003

[29] Kalantar B, Mansor SB, Shafri HZM, Halin AA. Integration of Template Matching and Object-based Image Analysis for Semi-automatic Oil Palm Tree Counting in UAV Images. In The 37th Asian Conference on Remote Sensing. 2017

[30] Hamedianfar A, Barakat A, Gibril M. Large-scale urban mapping using integrated geographic object-based image analysis and artificial bee

colony optimization from worldview-3 data. International Journal of Remote Sensing. 2019;**40**(17):1-26

[31] Kalantar B, Mansor SB, Sameen MI, Pradhan B, Shafri HZ. Drone-based land-cover mapping using a fuzzy unordered rule induction algorithm integrated into object-based image analysis. International Journal of Remote Sensing. 2017;**38**(8–10): 2535-2556

[32] Al-Ruzouq R, Shanableh A, Gibril BA, AL-Mansoori S. Image segmentation parameter selection and ant colony optimization for date palm tree detection and mapping from very-high-spatial-resolution aerial imagery. Remote Sensing. 2018;**10**(9): 1413

[33] Ahamed TN, Rao KG, Murthy JSR. GIS-based fuzzy membership model for crop-land suitability analysis. Agricultural Systems. 2000;**63**(2):75-95

[34] Davis TJ, Keller CP. Modelling uncertainty in natural resource analysis using fuzzy sets and Monte Carlo simulation: Slope stability prediction. International Journal of Geographical Information Science. 2000;**11**(5): 409-434

[35] Baidya P, Chutia D, Sudhakar S, Goswami C, Goswami J, Saikhom V, et al. Effectiveness of fuzzy overlay function for multi-criteria spatial modeling—A case study on preparation of land resources map for Mawsynram Block of East Khasi Hills District of Meghalaya, India. Journal of Geographic Information System. 2014; **6**(06):605

[36] Kalantar B, Pradhan B, Naghibi SA, Motevalli A, Mansor S. Assessment of the effects of training data selection on the landslide susceptibility mapping: A comparison between support vector machine (SVM), logistic regression (LR) and artificial neural networks (ANN). Geomatics, Natural Hazards and Risk. 2018;**9**(1):49-69

[37] Pradhan B, Seeni MI, Kalantar B. Performance evaluation and sensitivity analysis of expert-based, statistical, machine learning, and hybrid models for producing landslide susceptibility maps. In: Laser Scanning Applications in Landslide Assessment. Champions: Springer; 2017. pp. 193-232

[38] Hwang CL, Yoon K. Methods for multiple attribute decision making. In: Multiple Attribute Decision Making. Berlin, Heidelberg: Springer; 1981. pp. 58-191

[39] Yoon K. A reconciliation among discrete compromise solutions. Journal of the Operational Research Society. 1987;**38**(3):277-286

[40] Hwang CL, Lai YJ, Liu TY. A new approach for multiple objective decision making. Computers & Operations Research. 1993;**20**(8):889-899

[41] Ertuğrul İ, Karakaşoğlu N. Comparison of fuzzy AHP and fuzzy TOPSIS methods for facility location selection. The International Journal of Advanced Manufacturing Technology. 2008;**39**(7–8):783-795

[42] Seyedmohammadi J, Sarmadian F, Jafarzadeh AA, Ghorbani MA, Shahbazi F. Application of SAW, TOPSIS and fuzzy TOPSIS models in cultivation priority planning for maize, rapeseed and soybean crops. Geoderma. 2018; **310**:178-190

[43] Abdullahi S, Pradhan B, Mojaddadi H. City compactness: Assessing the influence of the growth of residential land use. Journal of Urban Technology. 2018;**25**(1):21-46

[44] Bui DT, Pradhan B, Lofman O, Revhaug I, Dick OB. Spatial prediction of landslide hazards in Hoa Binh province (Vietnam): A comparative

assessment of the efficacy of evidential belief functions and fuzzy logic models. Catena; 2012;**96**:28-40

[45] Erener A, Düzgün HSB. Improvement of statistical landslide susceptibility mapping by using spatial and global regression methods in the case of More and Romsdal (Norway). Landslides. 2010;**7**(1):55-68